

Passive Seismic Interferometry by Multi-Dimensional Deconvolution-Decorrelation

Carlos Almagro Vidal* and Kees Wapenaar, Delft University of Technology

INTRODUCTION

Seismic interferometrical methods enable the retrieval of reflection responses from the subsurface using ambient-noise recordings. The simplification under special conditions of wave-field reciprocity theorems shows how applying crosscorrelation of ambient-noise recordings between receivers may suffice to retrieve the reflection response of the subsurface as if virtual sources were located at the receiver locations where the recordings take place (Wapenaar & Fokkema, 2006; Schuster, 2009). Seismic interferometry (SI) by crosscorrelation with ambient noise assumes sources to have the same power spectrum, to be mutually uncorrelated and homogeneously distributed in the subsurface for an optimal result. This approach has successfully been applied to real datasets (Draganov *et al.* 2009). The result is strongly dependent on the frequency content of the noise signal, the source characteristics and the distribution of sources in the subsurface. Nakata *et al.* (2011) improved the retrieval process in the presence of surface-wave noise, using SI by crosscoherence.

The employment of SI by multi-dimensional deconvolution on passive seismics was presented by Wapenaar *et al.* (2008). This work presented acoustic results isolating the incident fields in the correlation result. Using the free-surface related multiples not only for retrieval but for suppression, Groenestijn & Verschuur (2010) employed an iterative inversion procedure to reconstruct the reflection response for the primaries only in acoustic medium. Following time-gating procedure but applied on the record with transient signals, Nakata *et al.* (2013) used elastic one-way wavefields in a real dataset with transient sources. However, the limitation of the source distribution restrained the estimation of reflections.

This work proposes an inversion procedure to reconstruct the reflection response without free-surface multiples, avoiding the need for estimation of the incident field neither in the correlation result nor in the record. The goal is to work with long ambient-noise data, minimising the effect of anisotropic illumination due to heterogeneities in the source distribution of the subsurface, and working independently of the ambient-source characteristics and power spectra. Results show the comparison of this method to the other SI methods with the increase of acquisition time in an acoustic medium. An extension for an elastic medium is presented making use of particle velocity components only and illumination diagnosis for preventing disturbing contributions from surface waves.

METHOD

Making use of the reciprocity relation of the convolution type for one-way wavefields, the relation between reflection and transmission responses with and without free-surface multiples for a given inhomogeneous medium enclosed by an upper boundary $\partial\mathbb{D}_0$ either at or below the free surface, and an

arbitrary lower boundary $\partial\mathbb{D}_m$ is (Wapenaar *et al.* 2004):

$$-\hat{G}_0^-(\mathbf{x}_A, \mathbf{x}_B, \omega) = -\hat{G}^-(\mathbf{x}_A, \mathbf{x}_B, \omega) + \int_{\mathbf{x} \in \partial\mathbb{D}_0} \hat{R}_0^\sim(\mathbf{x}_A, \mathbf{x}, \omega) \hat{G}^+(\mathbf{x}, \mathbf{x}_B, \omega) d^2\mathbf{x}. \quad (1)$$

This expression is described following the unified one-way wave equation in the space-frequency domain, where $\hat{G}^\pm(\mathbf{x}_A, \mathbf{x}_B, \omega)$ is the acoustic flux-normalized transmission response including both internal and free-surface multiples for a source at \mathbf{x}_B in the subsurface and a receiver at \mathbf{x}_A , at $\partial\mathbb{D}_0$. Superscripts refer to receiver wavefields (minus for upgoing,

and plus for downgoing). \hat{R}_0^\sim and \hat{G}_0^- are the reflection and transmission responses of the inhomogeneous medium with internal multiples but without free-surface multiples, and ω represents angular frequency. The integration over $\partial\mathbb{D}_0$ represents a convolution of the downgoing wavefield with the reflection response without free-surface multiples over receivers at \mathbf{x} at the upper boundary of the medium. This representation assumes the source at \mathbf{x}_B located just below the lower boundary $\partial\mathbb{D}_m$ and the medium to be homogeneous below it. However, this representation does not vary when the source is located at \mathbf{x}_B inside the medium \mathbb{D} . Applying this configuration ($\mathbf{x}_B \in \mathbb{D}$), but using the reciprocity relation of the correlation type instead, the representation result yields:

$$-\hat{G}_0^-(\mathbf{x}_A, \mathbf{x}_B, \omega) = -\{\hat{G}^+(\mathbf{x}_A, \mathbf{x}_B, \omega)\}^* + \int_{\mathbf{x} \in \partial\mathbb{D}_0} \hat{R}_0^\sim(\mathbf{x}_A, \mathbf{x}, \omega) \{\hat{G}^-(\mathbf{x}, \mathbf{x}_B, \omega)\}^* d^2\mathbf{x} - \int_{\mathbf{x} \in \partial\mathbb{D}_m} \hat{G}_0^-(\mathbf{x}_A, \mathbf{x}, \omega) \{\hat{G}^+(\mathbf{x}, \mathbf{x}_B, \omega)\}^* d^2\mathbf{x}, \quad (2)$$

where the last integration represents the contribution from the lower boundary $\partial\mathbb{D}_m$. In practical use, we cannot estimate the lower boundary quantity. Therefore, for practical considerations we ignore this term from here onward. This is approximately justified when the medium is strongly reflective below \mathbf{x}_B (Wapenaar, 2006). Equations 1 and 2 can be rewritten in the matrix notation of Berkhout (1982) as:

$$-\hat{\mathbf{G}}_0^- = -\hat{\mathbf{G}}^- + \hat{\mathbf{R}}_0^\sim \hat{\mathbf{G}}^+ \quad (3)$$

$$-\hat{\mathbf{G}}_0^- = -\{\hat{\mathbf{G}}^+\}^* + \hat{\mathbf{R}}_0^\sim \{\hat{\mathbf{G}}^-\}^* - \left(\hat{\mathbf{G}}_0^- \{\hat{\mathbf{G}}^+\}^* \right)_{\partial\mathbb{D}_m} \quad (4)$$

Neglecting the lower boundary $\partial\mathbb{D}_m$ term, one can eliminate the term $\hat{\mathbf{G}}_0^-$ by combining these two expressions together. The result for the reflection response is then represented by:

$$\hat{\mathbf{R}}_0^\sim = \left(\{\hat{\mathbf{G}}^+\}^* - \hat{\mathbf{G}}^- \right) \left(\{\hat{\mathbf{G}}^-\}^* - \hat{\mathbf{G}}^+ \right)^{-1}. \quad (5)$$

Passive Seismic Interferometry by Multi-Dimensional Deconvolution-Decorrelation

Now this expression is stabilized using least-squares regularization, and is represented by:

$$\begin{aligned} \hat{\mathbf{R}}_0^\sim &= \\ &\left(\{\hat{\mathbf{G}}^+\}^* \{\hat{\mathbf{G}}^-\}' + \hat{\mathbf{G}}^- \{\hat{\mathbf{G}}^+\}^\dagger - \hat{\mathbf{G}}^- \{\hat{\mathbf{G}}^-\}' - \{\hat{\mathbf{G}}^+\}^* \{\hat{\mathbf{G}}^+\}^\dagger \right) \\ &\left(\{\hat{\mathbf{G}}^-\}^* \{\hat{\mathbf{G}}^-\}' + \hat{\mathbf{G}}^+ \{\hat{\mathbf{G}}^+\}^\dagger - \hat{\mathbf{G}}^+ \{\hat{\mathbf{G}}^-\}' - \{\hat{\mathbf{G}}^-\}^* \{\hat{\mathbf{G}}^+\}^\dagger + \epsilon \mathbf{I} \right)^{-1}, \end{aligned} \quad (6)$$

where \dagger is complex conjugation and matrix transposition, \mathbf{I} is an identity matrix and ϵ is a stabilization parameter. Because of the correlation reciprocity relation, the estimation of

$\hat{\mathbf{R}}_0^\sim$ assumes the medium to be lossless and neglects evanescent waves. Since this expression results from the combination of the convolution and correlation reciprocity theorems, the reflection response obtained is the result of a "Multi-Dimensional Deconvolution-Decorrelation" (MD^3).

It is important to point out that the representation of $\hat{\mathbf{R}}_0^\sim$ in expression 6 is composed of four matrix products for both the normal and inverse operators. Two of these matrix products are crosscorrelation products, while the other two are cross-convolution products. During the reflection response estimate all the information is provided by the crosscorrelation products. If the medium is strongly reflective below where the passive source is located in \mathbb{D} , the cross-convolution products in expression 6 are not coherent and bring regularization to the inversion process. When this is not the case, the cross-convolution products will produce coherent artefacts accounting for the energy that left through the lower boundary $\partial\mathbb{D}_m$. If we want our representation to be consistent, we ought to include the contribution brought by the integration in equation 2 that we neglected, $\int_{\partial\mathbb{D}_m} \hat{\mathbf{G}}_0^- \{\hat{\mathbf{G}}^+\}^*$, because this lower boundary integration is responsible to cancel the artefacts produced due to the lack of reflectivity of the medium below the passive-source location.

However, one could reduce the appearance of these artefacts by ignoring the cross-convolution products in 6. This truncation, though, will require a larger regularization during the inversion process.

For the elastodynamic 2D situation, $\hat{\mathbf{G}}^\pm$ is subdivided by (Wapenaar *et al.* 2011):

$$\hat{\mathbf{G}}^\pm = \begin{pmatrix} \hat{\Phi}^\pm \\ \hat{\Psi}^\pm \end{pmatrix} \quad (7)$$

where Φ and Ψ stand for the pressure- and shear-, flux-normalized wavefields, respectively. The term $\hat{\mathbf{R}}_0^\sim$ can then be written as:

$$\hat{\mathbf{R}}_0^\sim = \begin{pmatrix} \hat{\mathbf{R}}_0^{\Phi,\Phi} & \hat{\mathbf{R}}_0^{\Phi,\Psi} \\ \hat{\mathbf{R}}_0^{\Psi,\Phi} & \hat{\mathbf{R}}_0^{\Psi,\Psi} \end{pmatrix} \quad (8)$$

where $\hat{\mathbf{R}}_0^{\Psi,\Phi}$, is the reflection response of the medium in \mathbb{D} in terms of a downgoing Φ -type wavefield at the source position and an upgoing Ψ -type wavefield at the receiver location.

RESULTS

We tested the new method together with the crosscorrelation and crosscoherence methods, in the heterogeneous 2D model displayed in Figure 1a. Receivers are located at 10 m depth from the surface.

Ambient-noise sources effectively surround the acquisition array. In the synthetic noise modelling sources are blended, being active every 2.5 s at random locations of the source-surrounding boundary. The occurrence of a noise source at the same location in the subsurface varied between once and 60 times during a total of 52 minutes of noise generated. The source signal is 10 s long for all sources, and they are uncorrelated one to another. All sources are dipoles, each one of them with a random orientation but with equal amplitudes. A representation of this is given in Figure 1a, where the source locations are represented with arrows (aiming on the dipole direction of the last source occurring at that location), and their size is proportional to the total occurrence of different sources at that same location. The maximum frequency in the sources' spectra varied from 6 to 40 Hz. The different colours of the arrows in Figure 1a represent the different maximum frequency of the spectrum of the last source that happened at that location (continuous colour scale from light yellow -for the highest maximum frequency- to black -for the lowest-).

The method was tested in both acoustic and elastic media. In both cases, the noise was processed in time windows of 16 s with 8 s overlap. Figure 1 shows the evolution of the result by using the same input data and applying three different SI methods: crosscoherence (CCh), crosscorrelation (CC) and multi-dimensional deconvolution-decorrelation (MD^3). The synthetic data was designed aiming to break all the assumptions under which SI by crosscorrelation and crosscoherence are valid. Yet, CC and CCh results were improved by means of reciprocity properties (adding causal and time-reversed retrieved parts together) and illumination diagnosis (Almagro Vidal *et al.* 2011). These additional processes helped these two approaches to compensate for the heterogeneous source distribution and source location occurrence. Results displayed in Figure 1 made use of three different amounts of noise employed in the reflection response retrieval: 2 minutes, 5 minutes and 52 minutes of continuous noise. Despite the directional balancing from illumination diagnosis, Figures 1c, 1f and 1i show the SI by crosscoherence results do not improve significantly regardless the amount of noise employed. Figures 1d, 1g and 1j reveal the same experience for SI by crosscorrelation. This is not the case in Figures 1e, 1h and 1k, where the quality of the response estimate increases with larger amount of noise employed, regardless of the frequency content of the signal or the occurrence of the source location.

Passive Seismic Interferometry by Multi-Dimensional Deconvolution-Decorrelation

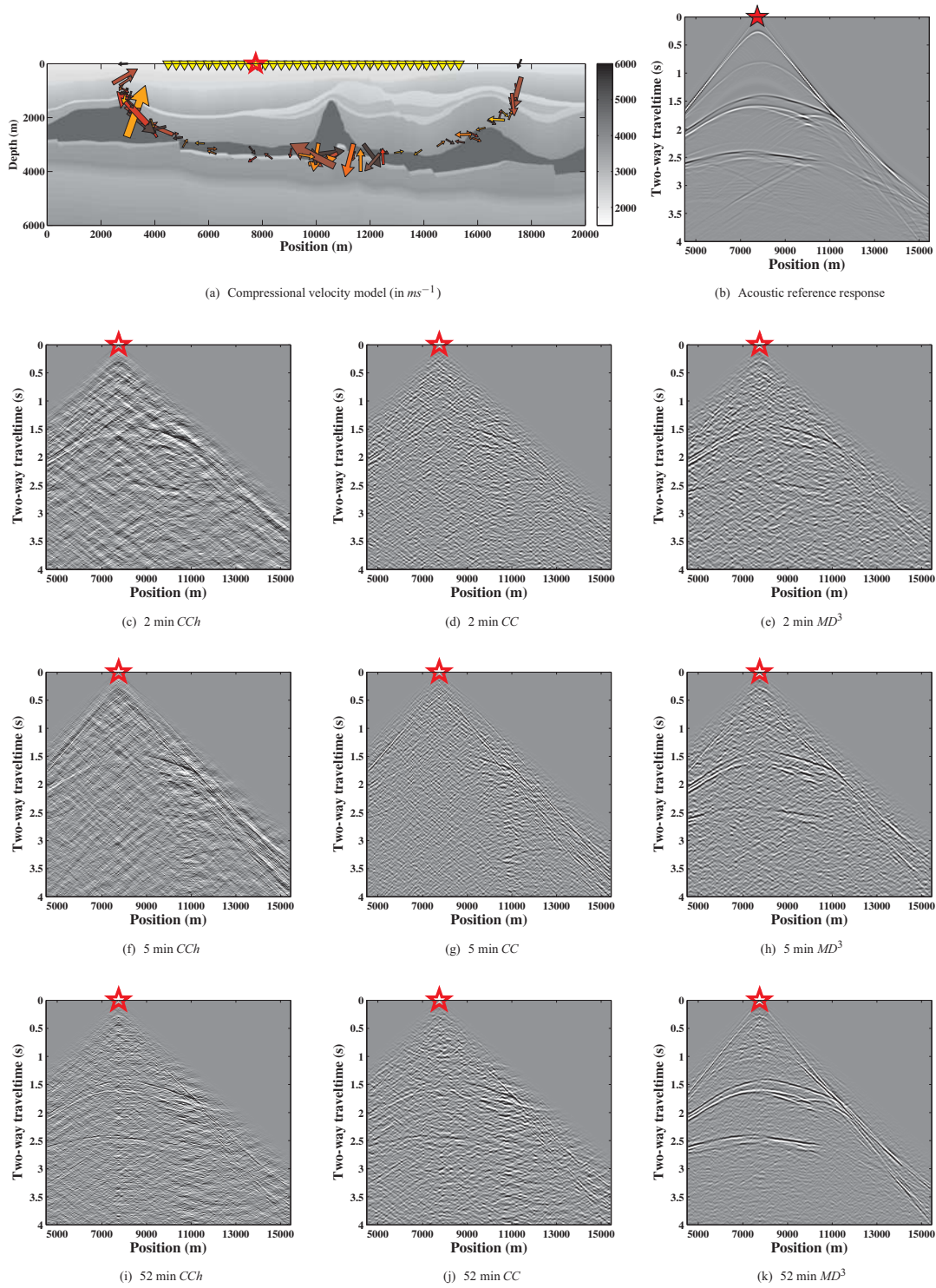


Figure 1: Results of different SI methods for passive seismics with acoustic ambient noise. (a) P-wave velocity model, with dipole noise sources with random spectra random directivity and irregular occurrence. (b) Directly modelled reflection response for an active source at $x_A = 7750$ m (the red open star in (a)). (c), (d) and (e) Retrieved virtual common-source gather at the same location using 2 minutes of noise, obtained using crosscoherence (c), crosscorrelation (d) and MD^3 (e). (f), (g) and (h) Same as in (c), (d) and (e), after 5 minutes of noise. (i), (j) and (k) Retrieved results after 52 minutes of noise.

Passive Seismic Interferometry by Multi-Dimensional Deconvolution-Decorrelation

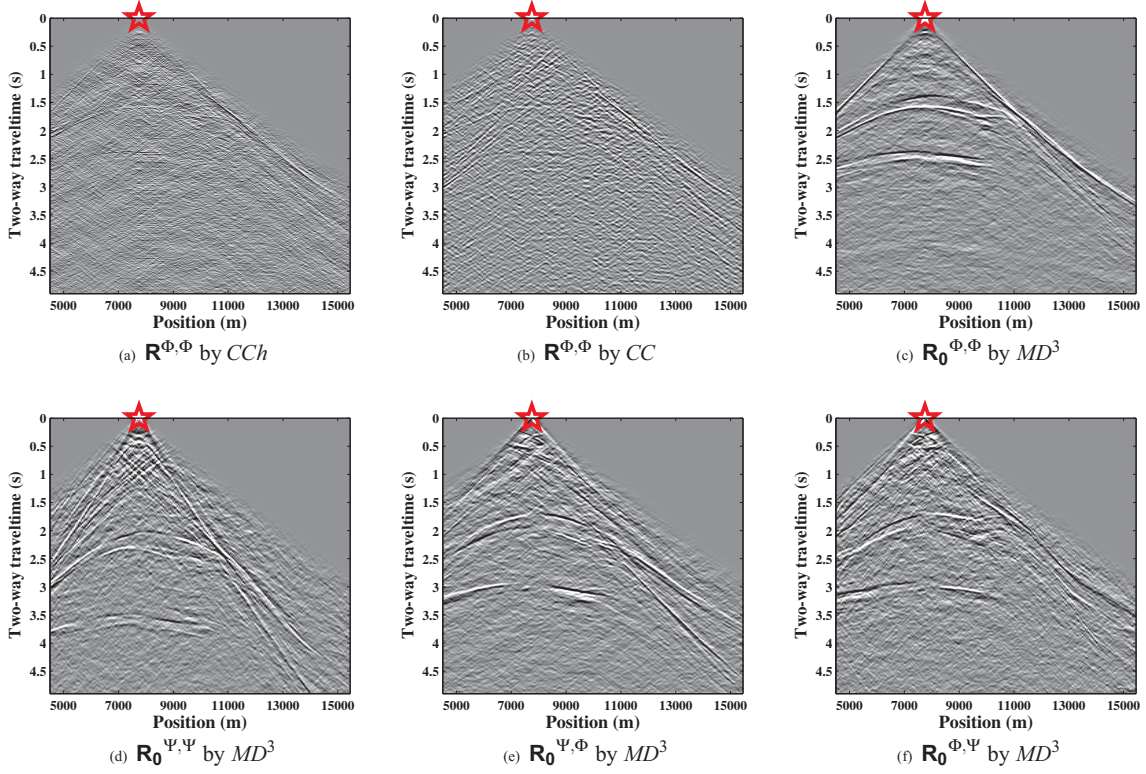


Figure 2: Reflection responses retrieved from the same model and location, source distribution and characteristics, as in Figure 1, but in an elasto-dynamic situation, with 52 minutes of ambient noise. (a), (b) and (c) Retrieved reflection responses obtained using SI by crosscoherence ($\mathbf{R}^{\Phi,\Phi}$), crosscorrelation ($\mathbf{R}^{\Phi,\Phi}$) and MD^3 ($\mathbf{R}_0^{\Phi,\Phi}$), respectively. (d), (e) and (f), $\mathbf{R}_0^{\Psi,\Psi}$, $\mathbf{R}_0^{\Psi,\Phi}$ and $\mathbf{R}_0^{\Phi,\Psi}$ responses resulting from employing SI by MD^3 .

In an elastic medium we employ only vertical and horizontal particle velocities, and make use of the elastic flux-normalized one-way wavefield decomposition described in Grobbe *et al.* (2013). In order to approach it to realistic conditions, some sources at or near the surface may contribute to surface waves to show up in the recordings. Therefore, we combine the method with illumination diagnosis previously applied with respect to the elastic decomposition, and analyse by time windows. The time windows with surface waves are dismissed for decomposition and further processing. Figure 2 shows the elastic results, which look very promising despite the approach employed during decomposition (using only particle velocity components detached from the free surface) and the nature of sources applied (only dipoles). The least-squares implementation runs under the condition that both sorts of sources are present in the data before the inversion is carried out. In this respect, we believe results may improve the moment different source types are included in the noise recordings (multicomponent stress sources in addition to the dipole sources).

CONCLUSIONS

We propose a method to retrieve the reflection response of the subsurface without free-surface multiples by using continuous noise recordings. The method makes use of one-way wavefields and does not require any time-gating for estimation of incident wavefields. In comparison with other interferometrical methods for reflection passive seismics, our method deals in a better manner with the source nature of the ambient noise, the heterogeneous frequency content of the ambient-noise signal, and compensates for uneven illumination by the subsurface noise sources. In addition, we profit from elastic one way wavefield decomposition methods using only particle velocities, in order to retrieve the elastic wavemodes from the reflection response.

ACKNOWLEDGEMENTS

We are specially thankful to Dr. J. Thorbecke, for providing his finite-difference code to perform the numerical modelling.

Passive Seismic Interferometry by Multi-Dimensional Deconvolution-Decorrelation

REFERENCES

- Almagro Vidal, C., van der Neut, J., Drijkoningen, G., Draganov, D. and Wapenaar, K. [2011] Retrieval of reflections from ambient noise using the incident fields (point-spread function) as a diagnostic tool, 73rd annual EAGE meeting, Vienna, P-376.
- Berkhout, A.J. [1982] Seismic migration. Imaging of acoustic energy by wave field extrapolation, Elsevier.
- Draganov, D., Campman, X., Thorbecke, J., Verdel, A. and Wapenaar, K. [2009] Reflection images from ambient seismic noise, *Geophysics*, Vol. 74, A63-A67.
- Grobbe, N., Neut, J.R. van der and Almagro Vidal, C. [2013] Flux-normalized elastodynamic wavefield decomposition using only particle velocity recordings, 83rd SEG annual meeting, Houston, Texas USA.
- Groenstijn, G.J.A. and Verschuur, D.J. [2010] Estimation of primaries by sparse inversion from passive seismic data, *Geophysics*, Vol. 75, SA61-SA69.
- Nakata, N. and Snieder, R. [2013] Body-wave interferometry using local earthquakes with multi-dimensional deconvolution and wavefield decomposition at free surface, 83rd SEG annual meeting, Houston, Texas USA.
- Nakata, N., Snieder, R., Tsuji, T., Larner, K. and Matsuoka, T. [2011] Shear-wave imaging from traffic noise using seismic interferometry by cross-coherence, *Geophysics*, Vol. 76, SA97-SA106.
- Schuster, G. T. [2009] Seismic interferometry: Cambridge Press, ISBN-13:9780521871242.
- Wapenaar, K., van der Neut, J., Ruijgrok, E., Draganov, D., Hunziker, J., Slob, E., Thorbecke, J., and Snieder, R. [2011] Seismic interferometry by crosscorrelation and by multi-dimensional deconvolution: a systematic comparison: *Geoph. J. Int.*, Vol. 185, 1335-1364.
- Wapenaar, K., van der Neut, J. and Ruijgrok, E. [2008] Passive seismic interferometry by multidimensional deconvolution, *Geophysics*, Vol. 73, A51-A56.
- Wapenaar, K. [2006] Green's function retrieval by cross-correlation in case of one-sided illumination, *Geophys. Res. Lett.*, Vol. 33, L19304-1 - L19304-6.
- Wapenaar, K. and Fokkema, J. [2006] Green's function representations for seismic interferometry, *Geophysics*, Vol. 71, SI33-SI46.
- Wapenaar, K., Thorbecke, J., and Draganov, D. [2004] Relations between reflection and transmission responses of three-dimensional inhomogeneous media: *Geoph. J. Int.*, Vol. 156, 179-194.